AD-A133 860 MAGNETIC PROPERTIES OF COCL2-INTERCALATED GRAPHITE(U) 1/1
MASSACHUSETTS INST OF TECH CAMBRIDGE M ELAHY ET AL.
APR 83 AFOSR-TR-83-0764 F49620-83-C-0011

UNCLASSIFIED F/G 20/3 NL

END

FILMED
DTIC

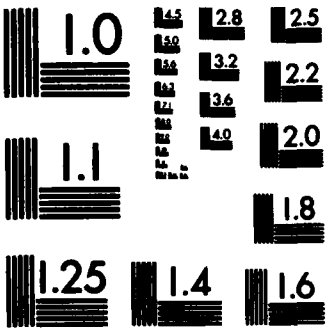

MICROCOPY RESOLUTION TEST CHART
NATIONAL BUREAU OF STANDARDS-1963-A

(2)

REPORT DOCUMENTATION PAGE

READ INSTRUCTIONS BEFORE COMPLETING FORM

1. REPORT NUMBER: AFOSR-TR- 83-0764	2. GOVT ACCESSION NO.: AD-A133 860
3. RECIPIENT'S CATALOG NUMBER	
4. TITLE (and Subtitle): MAGNETIC PROPERTIES OF $CoCl_2$-INTERCALATED GRAPHITE	5. TYPE OF REPORT & PERIOD COVERED: REPRINT
	6. PERFORMING ORG. REPORT NUMBER
7. AUTHOR(s): M. ELAHY, M. SHAYEGAN, K.Y. SZETO, G. DRESSELHAUS	8. CONTRACT OR GRANT NUMBER(s): F49620-83-C-0011
9. PERFORMING ORGANIZATION NAME AND ADDRESS: Massachusetts Institute of Technology, 77 Massachusetts Avenue, Cambridge, MA 02139	10. PROGRAM ELEMENT, PROJECT, TASK AREA & WORK UNIT NUMBERS: 61102F, 2306/C3
11. CONTROLLING OFFICE NAME AND ADDRESS: Air Force Office of Scientific Research/NE, Bolling AFB, DC 20332	12. REPORT DATE: April 1983
	13. NUMBER OF PAGES: 14
14. MONITORING AGENCY NAME & ADDRESS(if different from Controlling Office)	15. SECURITY CLASS. (of this report): Unclassified
	15a. DECLASSIFICATION/DOWNGRADING SCHEDULE

16. DISTRIBUTION STATEMENT (of this Report)

Approved for public release;
distribution unlimited.

17. DISTRIBUTION STATEMENT (of the abstract entered in Block 20, if different from Report)

18. SUPPLEMENTARY NOTES

Conference Proceedings, May 1983, Synthetic Metals (accepted for publication)
pages unknown

19. KEY WORDS (Continue on reverse side if necessary and identify by block number)

intercalated graphite
magnetic susceptibility
magnetic heat capacity
magnetic phase transitions
two-dimensional magnetism

20. ABSTRACT (Continue on reverse side if necessary and identify by block number)

See Over.

The temperature and magnetic field dependence of the magnetic susceptibility and heat capacity of graphite-$CoCl_2$ are investigated to understand the role of dimensionality in the observed magnetic phase transitions. The structure of graphite-$CoCl_2$ shows similarities between the magnetic layers of Co^{+2} in pristine and in the intercalated $CoCl_2$ compound. However, microstructural analysis shows the presence of small islands of magnetic ions. The theoretical model for the 2-dimensional planar magnets is extended to include small magnetic domains. The finite size effect analysis shows good agreement between the experimental and theoretical results. The presence of external magnetic fields demonstrates the static scaling hypothesis for the magnetic susceptibility and heat capacity.

Magnetic Properties of $CoCl_2$-Intercalated Graphite

M. Elahy,*§ M. Shayegan,†§ K.Y. Szeto*§ and G. Dresselhaus¶
Massachusetts Institute of Technology
Cambridge, MA 02139, USA

SUMMARY

The temperature and magnetic field dependence of the magnetic susceptibility and heat capacity of graphite-$CoCl_2$ are investigated to understand the role of dimensionality in the observed magnetic phase transitions. The structure of graphite-$CoCl_2$ shows similarities between the magnetic layers of Co^{+2} in pristine and in the intercalated $CoCl_2$ compound. However, microstructural analysis shows the presence of small islands of magnetic ions. The theoretical model for the 2-dimensional planar magnets is extended to include small magnetic domains. The finite size effect analysis shows good agreement between the experimental and theoretical results. The presence of external magnetic fields demonstrates the static scaling hypothesis for the magnetic susceptibility and heat capacity.

§Center for Materials Science and Engineering.
*Department of Physics.
†Department of Electrical Engineering and Computer Science.
¶Francis Bitter National Magnet Laboratory, sponsored by NSF.

INTRODUCTION

Intercalation of magnetic species into graphite provides an ideal system for the study of two-dimensional magnetism and for the investigation of the role of dimensionality in magnetic and structural properties. In these systems the interplanar interaction of magnetic spins can be systematically reduced by inserting a controlled number, n, of diamagnetic graphite layers between each adjacent pair of magnetic intercalate layers, where n is the stage index of the graphite intercalation compound (GIC).

Recent susceptibility measurements on $FeCl_3$-GIC, $CoCl_2$-GIC and $NiCl_2$-GIC have shown similarities in both the temperature and the magnetic field dependence of their magnetic behaviors [1]. It has furthermore been shown [2] that for these compounds the fit of the susceptibility above the critical region to a classical Curie-Weiss law is poor. A much better fit is obtained using the results of the Kosterlitz-Thouless theory (K-T) for the two-dimensional xy model [3].

We have chosen the $CoCl_2$-GIC system for a more critical investigation of this phase transition because it has the largest xy anisotropy in the spin-spin interaction among the known magnetic graphite intercalation compounds.

The lattice structure of pristine $CoCl_2$ is trigonal with space group $R\bar{3}m$, consisting of hexagonal layers of Co^{+2} in a triangular net separated from each other by two hexagonal layers of Cl^-. Pristine $CoCl_2$ undergoes an antiferromagnetic phase transition at the Neel temperature T_N = 24.9 K. For temperatures below T_N, the spins lie in the layer plane and align in two-dimensional ferromagnetic sheets which are stacked antiferromagnetically.

Experimental modeling of the neutron scattering experiments [4] have established values for the intraplanar and interplanar exchange energies of J = 28.5 K and J' = 2.2 K, with c-axis anisotropy energies of D = -16.0 K and D' = -3.3 K, respectively. The in-plane anisotropy field is estimated to be $H_A = 1.0 \times 10^{-2}$ T from the spin flop field $H_{SF} = 0.2$ T, and the saturation field $H_S = 3.3$ T [5].

This paper focusses on two important aspects of magnetic phase transitions in these magnetic GIC. The first topic concerns the finite size of the magnetic domains and its effect on the observed transition phenomena. The second topic concerns the role of an external magnetic field on the observed magnetic phenomena.

SAMPLE PREPARATION AND CHARACTERIZATION

Samples of graphite-$CoCl_2$ were prepared by the standard two-zone vapor transport method for graphite intercalation compounds [6,7]. Prior to heat treatment, the pristine $CoCl_2$ and the host HOPG sample were separated at a distance of a few cm inside a pyrex tube. Before sealing the ampoule, an atmosphere of Cl_2 (at ~ 350 torr pressure) and some $AlCl_3$ (~ 5% of $CoCl_2$ by weight) were added to the ampoule to act as a complexing halide [6]. The presence of this $AlCl_3$ was found to be crucial to the preparation of well-staged samples for $n > 2$. A two-zone furnace was used with the $CoCl_2$ heated to ~ 500 K and the HOPG to a slightly higher temperature. A larger temperature difference between the graphite and the $CoCl_2$ zones results in a higher stage of the intercalation compound. The intercalated samples were characterized for stage index and stage fidelity by (00ℓ) x-ray diffractograms.

To establish the role of the $AlCl_3$ complexing halide, we have done extensive structural characterizations of our samples. The results of these characterizations are presented here and are applied to the interpretation of the results of our magnetic measurements. The microstructure was examined using a scanning transmission electron microscope (STEM) and the presence of $AlCl_3$ was investigated by x-ray fluorescence techniques.

This analysis shows that $AlCl_3$ and $CoCl_2$ do not mix in the intercalated compound and each species forms its own domain. In Fig. 1(a) a typical (STEM) micrograph of the boundary of $CoCl_2$ and $AlCl_3$ is shown. The darker circular areas are $AlCl_3$ regions and the bright parts are $CoCl_2$ domains. Within the resolution of the x-ray fluorescence instrument, no Al was observed in the $CoCl_2$ domain and no Co in the $AlCl_3$ domain. Thus our system is modeled by small crystallites of staged, ordered $CoCl_2$-GIC. The measurement of the volume of intercalated $CoCl_2$ to the volume of intercalated $AlCl_3$ in the GIC samples is included in the analysis of our magnetic measurements. These stoichiometric determinations are done by chemical analysis of the bulk samples.

Figure 1(b) shows an electron diffractogram for the same sample as in Fig. 1(a). The diffractogram is interpreted as a superposition of pristine graphite spots, pristine $CoCl_2$ spots and rings whose radii match the lattice constants of $AlCl_3$ (see Fig. 1(c)). Thus the electron diffraction results further confirm the separation of $AlCl_3$ and $CoCl_2$ into distinct domains. The results further show an angular correlation between the $CoCl_2$ layer and the adjacent graphite, layers. The electron diffraction pattern implies a completely random angular distribution of the $AlCl_3$ planes, and indicates that the structure of $CoCl_2$ in $CoCl_2$-GIC is the same as in its pristine form. This experimental result indicates that the known in-plane magnetic parameters of pristine $CoCl_2$ and $CoCl_2$-GIC are nearly identical.

We also examined the structure of the $CoCl_2$ domains using the dark field image technique and found that these domains consist of small (100 Å x 500 Å) cigar shape islands which are uniaxially-oriented and containing ~9000 spins. Figure 1(d) shows a typical dark field image of $CoCl_2$ domains. The cigar shape of the domains is attributed to a minimization of the energy by aligning the maximum number of intercalate atoms over the hollows of the graphite honeycomb structure. The uniaxial orientation of the $CoCl_2$ domains allows for a high in-plane and c-axis packing density. Although the $CoCl_2$ remains incommensurate with the graphite substrate, this oriented needle-shaped domain arrangement creates an angular locking between the two lattices. This locking is also clear in the diffraction picture (Fig. 1(b)). The presence of these intercalant islands requires an extension of present 2-dimensional theories to include finite size effects, as discussed below.

In order to quantify our magnetic measurements, the chemical formulae $C_{\xi n}X$, where X stands for $(CoCl_2)_{1-y}$ $(AlCl_3)_y$ were determined from chemical analysis [8]. Using our (00ℓ) x-ray stage determination, the parameters ξ and y were found to be 7.07 and 0.68 respectively for the stage 4 compound. All compounds measured for stages n = 2, 3, 4, and 5 were found to yield ξ and y values in the range $7 < \xi < 8$ and $0.63 < y < 0.73$) [8].

RESULTS AND DISCUSSION

In Fig. 2a we plot our in-plane susceptibility results for stage 4 $CoCl_2$-GIC in the absence of an externally applied magnetic field. The shape of the temperature dependence has been shown to fit a two-dimensional model of the Kosterlitz-Thouless form [3]. The applicability of such a 2-D model to our system can be understood from the following considerations.

On the basis of our structural studies of graphite-$CoCl_2$, we can assume the following magnetic Hamiltonian for the system in the absence of an external magnetic field:

$$H = J \sum_{ij} S_i S_j + J_A \sum_{ij} S_i^z S_j^z + J' \sum_{ij} S_i S_k$$

where the values of the intraplane coupling constant J, and its associated anisotropy J_A are taken to be essentially the same as in the pristine $CoCl_2$ compound, i.e. J = 28.5 K and J_A = -16.0 K, respectively. The introduction of several diamagnetic graphite layers is expected to further decrease the already small value of J' in the pristine compound. In fact, our magnetic field dependent behavior of the susceptibility indicates that J'/J in a stage 2 compound has an upper bound of 2×10^{-4}. The dipole-dipole interaction for two spins separated by the adjacent magnetic layer distance in stage 2 gives a lower limit for this ratio of $\sim 6 \times 10^{-5}$ K.

In the high temperature phase characterized by unbound vortices, the K-T correlation length, ξ, increases with decreasing temperature. When ξ grows to $\sim a_o (J/J_A) = 1.3\, a_o$, where a_o is the lattice constant, the energy required to rotate a spin in the direction of the hard axis (c-axis) becomes of the same magnitude as J. Thus, below 28.5 K, where the thermal energy of the spins becomes less than the spin-spin coupling, we expect the spins to favor an xy system. On the other hand, at much lower temperatures, $\xi/a_o \sim (J/J')^{1/2} \sim 100$, and the effect of the adjacent magnetic plane is felt. If we assume that, on the average, each island contains less than 10^4 spins, then the system should satisfy the 2-D criterion throughout the critical region. We thus conclude that, in the temperature range of interest, the 2-D xy model is appropriate to the graphite-$CoCl_2$ system.

The Kosterlitz-Thouless theory for the two-dimensional xy model has been extended by Jose, Kadanoff, Kirkpatrick and Nelson (JKKN) to include the effect of the six-fold symmetry breaking anisotropy field [10]. They found that there exists a critical region in temperature with infinite initial susceptibility on both sides of which χ diverges as $\exp(b|t|^{-1/2})$. The upper temperature divergence of the susceptibility corresponds to a K-T type vortex binding-unbinding phase transition while the lower temperature divergence corresponds to a transition from the bound vortex state to a state with conventional long-range order.

The analysis of JKKN is valid only for $t < 0.1$ where $t = T/T_c - 1$. But we have extended the JKKN model to temperatures further above the upper phase transition temperature T_{c1} using the Nelson-Rudnick extension formalism and the high temperature 2-D Coulomb gas Green function. We found that the same functional form is applicable to a much larger temperature range, with the parameter b being weakly temperature dependent [9].

Thus the use of the exponential function to fit our experimental data over a wide temperature range as reported earlier can be theoretically justified. The same experimental situation has been reported for K_2CuF_4 [11]. We have also found, using numerical computation, that the rounding of χ at the susceptibility peak is consistent with a finite size analysis, using values for the island size found experimentally.

As reported previously [12] the magnetic heat capacity measurements are consistent with the Monte Carlo calculations based on the xy model [13]. Both experimental and theoretical results exhibit a broad peak slightly above the temperature of the phase transition from unbound to bound vortices.

The application of an external magnetic field (in-plane) has a dramatic effect on the magnetic properties. In the case of the susceptibility, small magnetic fields have significant effects, as shown in Fig. 2b where we plot χ vs. temperature for several values of the externally applied magnetic field H. As H increases, the magnitude of the susceptibility at the peak, χ_{max}, decreases, and the position of the peak in temperature, $T_{max}(\chi)$, shifts to higher temperatures.

In Fig. 3 we plot the field dependence of χ_{max} and T_{max} on a log-log scale. The data fit a power law of the form $\chi_{max}(H) \sim H^{-\lambda}$ where $\lambda = 0.80$. Similar magnetic field and temperature dependences have been reported by Suzuki and Ikeda in K_2CuF_4 [14], who have found agreement between their results and the static scaling hypothesis of Kadanoff [15]. The spin-spin interaction in K_2CuF_4 is primarily of the Heisenberg type with only 1% xy anisotropy and the in-plane symmetry-breaking field is negligible. Nevertheless, K_2CuF_4 and $CoCl_2$-GIC exhibit essentially identical behavior in the pertinent T and H ranges. The value of $\lambda = 0.82$ is obtained for K_2CuF_4 [14], in excellent agreement with our values for λ in $CoCl_2$-GIC.

Both the $\chi(T)$ and $C_M(T)$ measurements on $CoCl_2$-GIC show that T_{max} shifts to higher temperatures with increasing field as $T_{max}(H) - T_{max}(0) \sim H^{\mu}$ (see Fig. 3). From this plot we estimate the exponent μ from the magnetic field dependence of the maximum in χ to be $\mu = 0.37 \pm 0.05$ and from C_M to be $\mu = 0.9 \pm 0.3$. The discrepancy between the value of μ obtained from the field dependence of the susceptibility and of the heat capacity in the present work is not fully understood.

Our results indicate that in graphite-$CoCl_2$, when the amplitude of the external field exceeds the in-plane 6-fold symmetry breaking field of 100 Oe, the behavior of χ is also in good agreement with the static scaling hypothesis. Furthermore, the critical exponents in this magnetic field region are independent of stage index. This suggests that the interaction of a spin with the external field in this region dominates over the interplanar spin-spin interaction. This in turn suggests a maximum value of J' for the lowest stage (n = 2) which is $J'_{max} = 7 \times 10^{-3}$ K.

CONCLUSIONS

The experimental $CoCl_2$-GIC system provides an important experimental system for study of the 2-dimensional xy model. The static scaling hypothesis as well as finite size effects are introduced to interpret the measurements. This model yields excellent agreement with the experimental data.

ACKNOWLEDGMENTS

This work was supported by AFOSR contract #F49620-83-C-0011. We wish to thank Profs. M.S. Dresselhaus and R.J. Birgeneau for helpful discussions throughout this work. We would also like to express our appreciation to Dr. C.W. Lowe, and Ms. L. Salamanca-Riba for help with the sample preparation. We would also like to thank Dr. A.J. Garratt-Reed for his help with the STEM.

REFERENCES

1. M. Elahy, C. Nicolini, G. Dresselhaus, and G.O. Zimmerman, Solid State Commun. 41, 289 (1982).

2. M. Elahy and G. Dresselhaus, in Intercalated Graphite, edited by M.S. Dresselhaus, G. Dresselhaus, J.E. Fischer and M.J. Moran, (Elsiever, New York, 1983), vol. 20, p. 207.

3. J.M. Kosterlitz, J. Phys. C, Solid State Phys. 7, 1046 (1974).

4. M.T. Hutchings, J. Phys. C, Solid State Phys. 6, 3143 (1973).

5. L.J. de Jongh and A.R. Miedema, Advances in Physics 23, 1 (1974).

6. E. Stumpp, Mater. Sci. Engng. 31, 53 (1977).

7. A. Herold, in Phys. and Chem. of Materials with Layered Structures, Vol. edited by F. Levy (Dordrecht, Reidel), p. 323 (1979).

8. M. Shayegan, M.S. Dresselhaus, L. Salamanca-Riba, G. Dresselhaus, J. Heremans, and J-P. Issi, Phys. Rev. B27 xxxxx (1983); M. Shayegan, PhD. Thesis, MIT, 1983 (unpublished).

9. K.Y. Szeto (unpublished).

10. J.V. Jose, L. Kadanoff, S. Kirkpatrick and D.R. Nelson, Phys. Rev. B16, 1217 (1977).

11. K. Hirakawa, H. Yoshizawa and K. Ubukoshi, J. Phys. Soc. Jpn 51, 2151 (1982).

12. M. Shayegan, L. Salamanca-Riba, J. Heremans, G. Dresselhaus, and J-P. Issi, in Intercalated Graphite, edited by M.S. Dresselhaus, G. Dresselhaus, J.E. Fischer and M.J. Moran, (Elsiever, New York, 1983), vol. 20, p. 213.

13. J. Tobochnik and G.V. Chester, Phys. Rev. B20, 3761 (1979).

14. M. Suzuki and H. Ikeda, J. Phys. Soc. Jpn. 50, 1133 (1981).

15. L.P. Kadanoff, W. Gotze, D. Hamblen, R. Hecht, E.A.S. Lewis, V.V. Palciauskas, M. Rayl and J. Swift, Rev. Mod. Phys. 39, 395 (1967).

FIGURE CAPTIONS

Fig. 1.(a) STEM bright field image -The dark regions are $AlCl_3$ domains and the bright regions surrounding them are $CoCl_2$ domains. X-ray fluorescence shows no $CoCl_2$ in the $AlCl_3$ regions and no $AlCl_3$ in the $CoCl_2$ regions.

(b) Electron diffractogram of a graphite-$CoCl_2$ sample. To within our resolution, the pattern shows a super-position of HOPG and pristine $CoCl_2$ diffraction spots. Although $CoCl_2$ is incommensurate with the graphite substrate, a high degree of angular locking is observed between them, and hence the spot pattern. No such correlation is apparent between the graphite and $AlCl_3$ diffraction peaks which form circular rings with radii compatible with the inplane lattice constant of pristine $AlCl_3$.

(c) A schematic representation of the diffraction pattern of Fig. 1b.

(d) TEM dark field image of $CoCl_2$ diffracted light in graphite-$CoCl_2$. The $CoCl_2$ regions consist of needle shaped islands of 100A x 500A dimensions, uniaxially oriented to allow for maximum packing and a minimum in free energy.

Fig. 2. Temperature dependence of the in-plane susceptibility of stage 4 $CoCl_2$-GIC for (a) $H = 0$ and (b) for several external magnetic field values.

Fig. 3. Field dependence of the susceptibility peak amplitude χ_{max} (right scale), and of the shift in the susceptibility peak position $T_{max}(\chi)$ and the heat capacity peak position $T_{max}(C_M)$ (right scale).

(a)

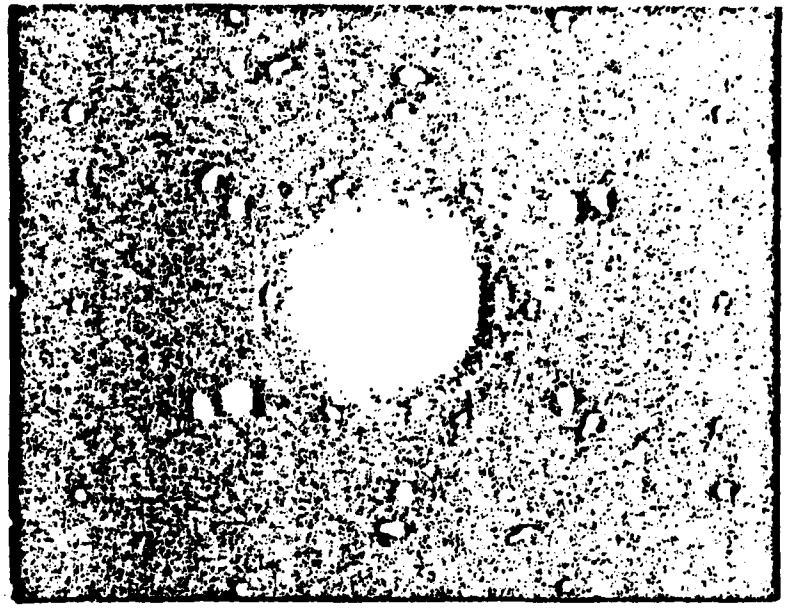

(b)

(d)

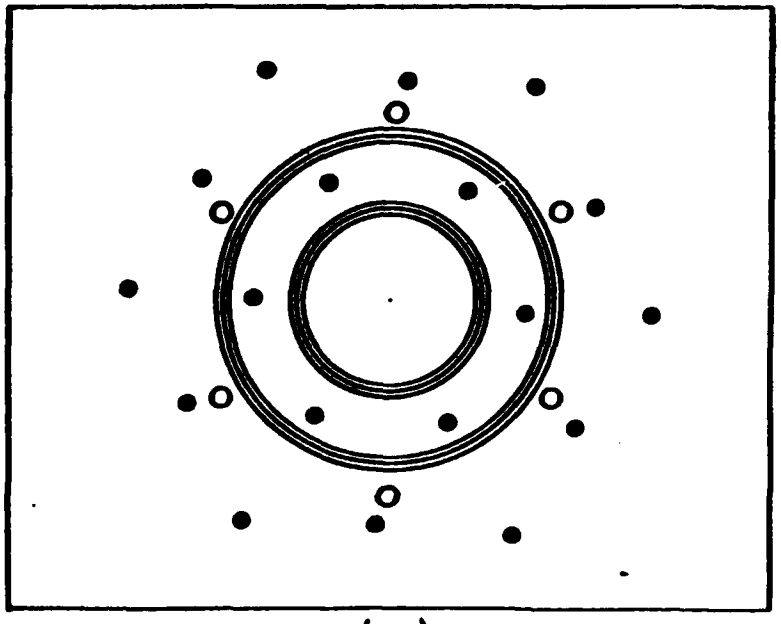

(c)

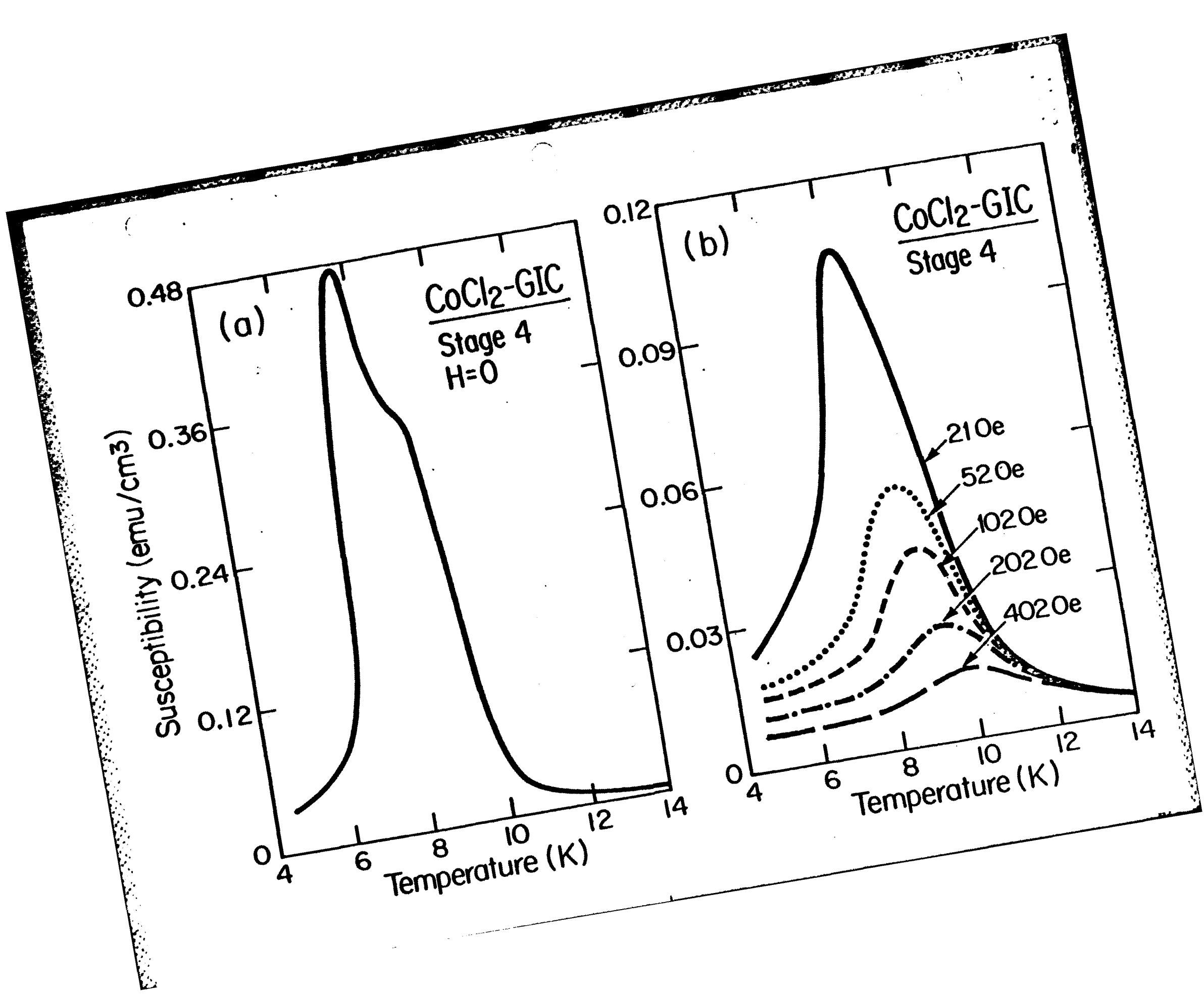
(a)
$CoCl_2$-GIC
Stage 4
H=0
Susceptibility (emu/cm³)
0.48
0.36
0.24
0.12
0
4
6
8
10
12
14
Temperature (K)
(b)
$CoCl_2$-GIC
Stage 4
0.12
0.09
0.06
0.03
0
21 Oe
52 Oe
102 Oe
202 Oe
402 Oe
4
6
8
10
12
14
Temperature (K)

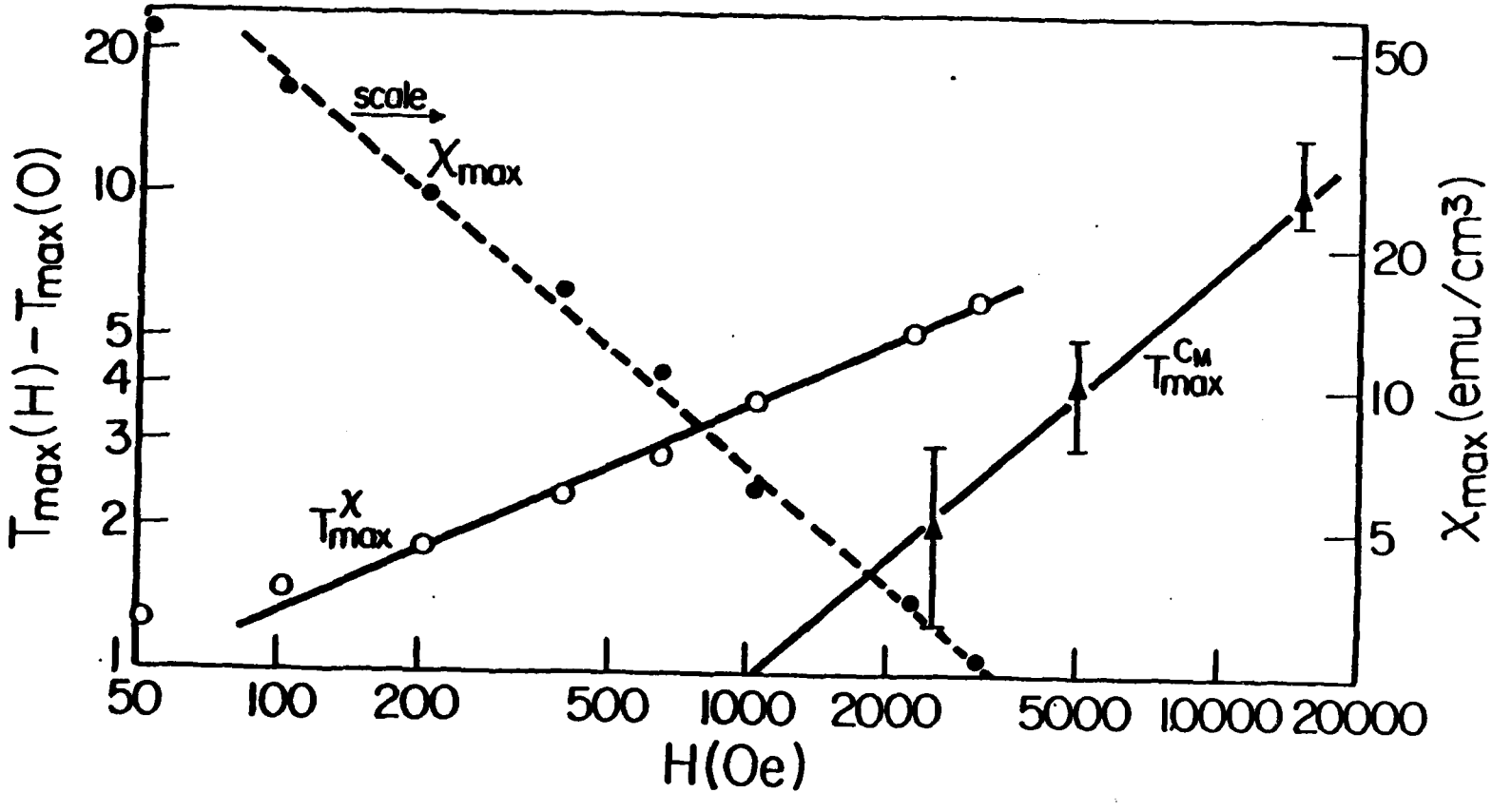
20
10
5
4
3
2
1
50
20
10
5
scale
χ_{max}
T_{max}^{χ}
$T_{max}^{C_M}$
$T_{max}(H) - T_{max}(0)$
χ_{max} (emu/cm^3)
50
100
200
500
1000
2000
5000
10000
20000
H(Oe)

Fig.

END

FILMED

11-83

DTIC